Polymer Chemistry

Cite this: *Polym. Chem.*, 2012, **3**, 685

www.rsc.org/polymers

**PAPER**

# One-pot synthesis of amphiphilic reversible photoswitchable fluorescent nanoparticles and their fluorescence modulation properties†

**Jian Chen,*[ab] Peisheng Zhang,[a] Gang Fang,[c] Chao Weng,[d] Jia Hu,[a] Pinggui Yi,*[a] Xianyong Yu[a] and Xiaofang Li[a]**

***Received 6th November 2011, Accepted 12th December 2011***
**DOI: 10.1039/c2py00525e**



In the present study, we report on the fabrication of novel amphiphilic reversible photoswitchable fluorescent nanoparticles by a facile one-pot miniemulsion polymerization using a biocompatible polymerizable nonionic surfactant, ω-methoxy poly(ethylene oxide) undecyl α-methacrylate (PEO-R-MA-40), in which spiropyran-linked methacrylate (SPMA) and the energy level well-matched fluorescent dyes: fluorescein-based, vinylic crosslinking monomer (fluorescein-*O*,*O*-bis-propene (FBP)) were covalently incorporated into polymeric matrix during the polymerization process. Under the alternative irradiation of UV and visible light, the fluorescent emission of FBP dye in nanoparticles can be reversibly modulated by cyclical transformation of spiropyran moieties' structure on the basis of intra-particle FRET process between FBP and merocyanine (MC) state of spiropyran. The as-prepared fluorescent nanoparticles display high dye load, as well as controllable amount and ratio of the two dyes because of covalent linkage between dye molecules and the particle. Moreover, the observed FRET efficiencies (66.3–98.5%) can be facilely tuned by controlling the amount (ratio) of the two chromophores. Overall, significant features of these novel amphiphilic reversible photoswitchable fluorescent nanoparticles include higher biocompatibility and photostability, relatively fast photoresponsivity and better photoreversibility as compared to some previous reported systems, which are promising for biological, optical fields and so on.

## Introduction

In the past decade, fluorescent nanoparticles have been of high interest in many biological applications,[1–6] since they exhibit several advantages over single dye molecules, such as increased brightness and reduced photobleaching.[7,8] In particular, fluorescent nanoparticles based on photochromic compounds (spiropyran), the fluorescence of which can be reversibly photoswitched through the structural inter-conversion between two states of spiropyran moieties in nanoparticles upon the irradiation of UV or visible light,[9,10] are more attractive because they can distinguish sites of interest from false positive signals generated by adventitious fluorescent biomolecules.[11,12] The additional advantages of these photoswitchable fluorescent nanoparticles can be not only greatly enhancing the fluorescence emission of hydrophobic fluorescent dyes in aqueous media, but also effectively avoiding drawbacks of fluorescent dyes for *in vivo* applications due to their cytotoxicity, pH-dependent fluorescence and so on.[13–15]

Conventional photoswitchable fluorescent nanoparticles generally fixed the dye molecules in the particle matrix by physical doping or adsorption during the synthesis process.[16,17] However, the slow release of fluorescent dyes during a synthesis or preservation process might be disadvantageous in terms of long-term stability. In addition, the leakage of unbound dyes is also a disadvantage for potential biological application. To address this issue, one promising strategy is to covalently incorporate dye molecules into polymer nanoparticles, which greatly reduces potential problems such as dye aggregation and dye leakage. To date, several studies have been devoted to

[a]*Key Laboratory of Theoretical Chemistry and Molecular Simulation of Ministry of Education, Hunan Province College Key Laboratory of QSAR/QSPR, School of Chemistry and Chemical Engineering, Hunan University of Science and Technology, 411201, China. E-mail: cj0066@gmail.com; pgyi@hnust.cn; Fax: +86 731-58290045; Tel: +86 731-58290045*
[b]*Key Laboratory of Advanced Functional Polymeric Materials, Xiangtan University, 411105, China*
[c]*College of Materials Science & Engineering, South China University of Technology, Guangzhou, 510640, China*
[d]*College of Chemistry, and Key Lab of Environment Friendly Chemistry and Application, Ministry of Education, Xiangtan University, Xiangan, 411105, China*

† Electronic supplementary information (ESI) available: $^1$H NMR spectra of FBP, SPMA monomer and PEO-R-MA-40 as well as its intermediate compounds. Detailed description of calculation of the fluorescence quantum yield of donor, the Förster radii ($R_0$), experimental energy transfer efficiency and estimation of donor–acceptor distance, and estimation of $N_A$ (number of NR residing around one donor within the effective energy transfer distance) *etc*. See DOI: 10.1039/c2py00525e

covalently incorporating both photochromic components and fluorescent dyes into nanoparticles to fabricate nanoparticle-based photoswitchable fluorescent systems by using various methods, such as microemulsion polymerization,[18] sol–gel synthesis,[19] atom transfer radical polymerization (ATRP)[20] and miniemulsion polymerization,[21] *etc.* It is noteworthy that the use of the ATRP method to covalently incorporate multiple dyes into nanoparticles needs relatively complicated routes; while the microemulsion polymerization or sol–gel approaches are not usually able to effectively control the quantity or ratio of dyes in nanoparticles due to the different diffusion coefficients in water (or another liquid phase) between the dyes and monomer during the preparation process. In contrast, the covalent incorporation of dyes in nanoparticles using the miniemulsion polymerization approach should be able to provide many advantages, including facile and flexible synthesis route, high dye loading, enhanced dye stability, controllable quantity and ratio of dyes *etc.*[21]

It is well known that surfactant plays a significant role in miniemulsion polymerization and later in storage.[22–25] Surfactant can be used in sufficient quantity to stabilize the monomer droplets, so as to prevent these droplets from coalescing.[23,26,27] Traditional miniemulsion polymerization generally employs the anionic surfactant sodium dodecyl sulfate (SDS) as emulsifier to stabilize the latexes and control the particle size. It has been found that SDS works as a high-efficiency emulsifier in the preparation of nanoparticles by this polymerization technique.[24–28] Despite the huge advantage of SDS, the migration or desorption of its ionic groups from the product might be disadvantageous in terms of long-term stability.[25] To avoid these negative features of conventional surfactants, the recently developed polymerizable nonionic surfactants (so-called surfmers), which are not physically adsorbed but covalently bonded onto the surface of latex particles, have attracted much attention due to their advantages over non-polymerizable anionic surfactants (SDS): (i) the latex products stabilized by nonionic surfactants are quite insensitive to changes in the ionic strength of the aqueous solution;[29] (ii) the properties of the resulting latexes such as resistance to freeze–thaw cycles are significantly improved;[30,31] (iii) the template effect of the amphiphilic interface may be better persevered during the polymerization process.[25,32] Among various polymerizable nonionic surfactants, the biocompatible amphiphilic poly(ethylene oxide) (PEO) macromonomer (PEO-R-MA-40) has been developed to serve as a promising candidate to stabilize the latexes.[33,34] Moreover, the long PEO groups of PEO-R-MA-40 anchored on the surface of latex particles provide a permanent steric stabilization for the long-term stability of latexes. Although extensive work based on PEO-R-MA-40 has been reported for dispersion polymerization,[35,36] emulsion polymerization,[33] microemulsion copolymerization[37,38] and so forth, there is little information about miniemulsion polymerization to the best of our knowledge.

In this work, we have prepared novel amphiphilic reversible photoswitchable fluorescent nanoparticles *via* covalent incorporation with the fluorescent vinylic crosslinking monomer, fluorescein-*O*,*O*-bis-propene (FBP) and spiropyran-linked methacrylate (SPMA) using a facile one-pot miniemulsion polymerization in the presence of PEO-R-MA-40 as a polymerizable nonionic surfactant. Among various classical luminophores, fluorescein derivatives with their bright color and fluorescence, have been widely used for colouring polymers, food, cosmetics, pharmaceuticals and in laser techniques.[39–43] Despite the large amount of work on the fluorescein derivatives, little is known about their application in photoswitchable fluorescent nanoparticles as fluorescent donor. For this approach, the two energy level-matched chromophores, with their amount and ratio being well controllable, can be covalently linked to the polymeric matrix during the polymerization process, which can greatly increase the stability of photoswitchable fluorescent nanoparticles. The fluorescence emission of FBP dye in nanoparticles can be reversibly switched "on" and switched "off" as a result of the structural inter-conversion between two states of spiropyran moieties upon UV and visible light irradiation (Scheme 2). Moreover, these novel amphiphilic reversible photoswitchable fluorescent polymeric nanoparticles also exhibit other advantages, such as improved biocompatibility and environmental stability, tunable FRET efficiency, relatively fast photoresponsibility and better photoreversibility compared to our previously reported systems.[16,21]

## Experimental

### Materials

The poly(ethylene glycol) methyl ether (PEOH-40, $M_w$ = 1900, Alfa), 3,4-dihydro-2*H*-pyran (DHP, Aladdin), 11-bromoundecanol (Fluka), p-toluenesulfonic acid monohydrate (98%, TCI), methacryloyl chloride (MAC, 97%, Aladdin), fluorescein (TCI), 18-crown-6 (99%, Aladdin), allyl bromide (98%, Aladdin), n-hexadecane (HD, 99%, Aldrich), N,N′-dicyclohexylcarboiimide (DCC, 99%, Alfa), and 4-dimethylamino-pyridine (DMAP, 99%, Alfa) were used as received. Dichloromethane (A.R.) was washed with sulfuric acid and then distilled from $CaH_2$. 2-Hydroxyethyl methacrylate (HEMA, 97%, Aldrich) was dissolved in water (25 vol%) and washed four times with an equal volume of hexane, then dried over $MgSO_4$ and distilled under vacuum prior to use. Potassium persulfate (KPS, 99.99%, Aldrich) was recrystallized from water and dried under vacuum. The water used in this work is double-distilled water which was further purified with a Milli-Q system. Tetrahydrofuran (THF, A.R.), acetonitrile (A.R.) and triethylamine (A.R.) were distilled over $CaH_2$. Petroleum ether, benzene, and other reagents were analytical reagents and used without further purification.

### Measurements

$^1$H NMR spectra were recorded on a Bruker Avance 500 MHz NMR spectrometer. The nanoparticle diameters were determined by a Malvern Nano-ZS90 instrument and their morphology was observed with an atomic force microscope (AFM, Veeco Nanoman VS) in the tapping mode. UV-Vis spectra were recorded on a Shimadzu UV-2501PC spectrophotometer at room temperature. Fluorescence spectra were recorded on a Shimadzu RF-5301PC fluorescence spectrophotometer at room temperature.

### Synthesis of the PEO-R-MA-40 macromonomer

A four-step procedure was required to obtain PEO-R-MA-40 according to a modified procedure described in the literature.[34]

 

The entire synthesis is outlined in Scheme 1, and the detailed synthetic routes are shown in the ESI†.

### Synthesis of the fluorescein-o,o-bis-propene (FBP) monomer

Synthesis was carried out according to a modified procedure described in the literature.[39,40] Allyl bromide (0.01 mol) was added dropwise to a mixture of 0.005 mol of fluorescein in 100 ml acetonitrile, 0.0005 mol of 18-crown-6 and 0.013 mol of finely ground potassium hydroxide at room temperature. The resulting mixture was stirred under reflux for 2 h, after which the organic phase was filtered and the organic solvent evaporated under vacuum, then the residues were purified by silica gel column chromatography using dichloromethane (v/v) as eluent to afford FBP (78% yield). $^1$H NMR spectrum for the product is shown in Fig. S2 (ESI).† (500 MHz, $CDCl_3$, 25 °C) $\delta$: 4.46 (d, 2H, –$OCH_2$– of ether), 4.65 (d, 2H, –$OCH_2$– of ester), 5.08–5.12 (m, 2H, =$CH_2$ of ether), 5.36–5.48 (m, 2H, =$CH_2$ of ester), 5.56–5.62 (m, 1H, =CH– of ether), 6.03–6.09 (m, 1H, =CH– of ester), 6.45–8.26 (m, 10H, aromatic protons).

### Synthesis of the spiropyran-linked methacrylate (SPMA) monomer

SPMA were synthesized with a slightly modified procedure reported elsewhere.[16] During the synthesis process, all the reaction vessels were wrapped with aluminum foil, so as to ensure the reaction was performed in the dark. For the synthesis of SPMA, firstly, l-(β-carboxyethyl)-3′,3′-dimethyl-6-nitrospiro(indoline-2′,2-chromane) (SPCOOH) was synthesized according to a literature procedure.[44] Subsequently, SPCOOH (3.8 g, 10 mmol), HEMA (3.9 g, 30 mmol) and DMAP (0.27 g, 2 mmol) were added to a 250 ml round-bottomed flask equipped with a pressure-equalized dropping funnel, magnetic stirrer and a nitrogen inlet. Cold dry THF (100 ml) was added to the flask and the solution was cooled to 0 °C, a red brown solution resulted. DCC solution (2.06 g, 10 mmol in THF) was added to the resulted solution *via* the pressure-equalized dropping funnel over 45 min. The flask was maintained at 0 °C for 2 h, then the temperature was raised gradually to room temperature about 24 h. The product was filtrated with cold dry THF (100 ml) three times giving a red filtrate. After removal most of the solvent under vacuum distillation, the residue was washed by larger amount of distilled water to remove the unreacted HEMA. The precipitate was dissolved in benzene and filtrated again to remove the unreacted SPOOH, afterwards most of the solvent was evaporated under vacuum and below 45 °C for avoiding SPMA polymerization, the solution was precipitated in a large amount of petroleum ether, finally a fine red-purple precipitate of purified 2-(3-(3′,3′-dimethyl-6-nitrospiro(indoline-2′,2-hromane)-1′-yl)propanoyloxy)-ethyl-methacrylate (SPMA) was obtained. The target product was dried in vacuum oven overnight at room temperature. The product was red purple powder in 85% yield. $^1$H NMR spectrum for the product is shown in Fig. S3 (ESI).† (500 MHz, $CDCl_3$, 25 °C). $\delta$: 1.0–1.3 (ds, 6H, $CH_3$ of spiropyran), 1.8–1.9 (s, 3H, $CH_3$ of HEMA, connected to olefinic carbon), 2.6–2.7 (m, 2H, –$CH_2$COO– of spiropyran), 3.5–3.6 (m, 2H, –$CH_2$N– of spiropyran), 4.2 (dt, 4H, –$CH_2$O– of HEMA), 5.5–6.0 (m, 4H, olefinic protons, $CH_2$ and two CH), 6.6–8.1 (m, 7H, aromatic protons).

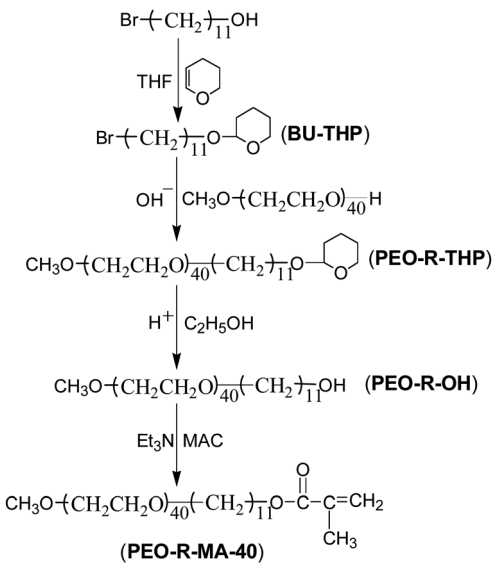


**Scheme 1** Synthesis of PEO-R-MA-40.

### Synthesis of novel amphiphilic reversible photoswitchable fluorescent nanoparticles

A mixture containing the monomers and hydrophobes (MMA, FBP, SPMA, HD) was added to water solution with polymerizable surfactant (PEO-R-MA-40) and stirred (1000 r/min) for 10 min, then, the mixture was ultrasonicated for 30 min (KQ2000DE) to obtain a miniemulsion. The mixture was cooled in an ice-bath during ultrasonication to avoid being heated. The resulting miniemulsion was put into a 50 ml flask equipped with a condenser, which was immersed in an oil bath with a thermostat. The polymerization was started by adding aqueous solution of KPS and preceded at 60 °C for 180 min. After the polymerization, the as-prepared nanoparticle dispersions were percolated and finally the novel nanoparticles dispersions were obtained.

## Results and discussion

### Synthesis of polymerizable nonionic surfactant PEO-R-MA-40

The macromonomer PEO-R-MA-40 was synthesized as described in the ESI,† in basic conditions (Scheme 1). Firstly, DHP was used to protect the hydroxyl group of 11-bromoundecano1, and it was then reacted with poly(ethy1ene glycol) methyl ether to give the intermediate PEO-R-THP through a modified Williamson reaction. Subsequently, the hydrolysis of the THP-ether to the corresponding alcohol (PEO-R-OH) was carried out. The final introduction of a methyl acrylate group to PEO-R-OH produced the unsaturated double bond containing macromonomer (PEO-R-MA-40). Their $^1$H NMR spectra are displayed in Fig. S1 (ESI).†

### Preparation of novel amphiphilic reversible photoswitchable fluorescent polymeric nanoparticles by using PEO-R-MA-40.

In the present work, novel amphiphilic reversible photoswitchable fluorescent nanoparticles were prepared by a facile

one-step miniemulsion polymerization using PEO-R-MA-40. The macromonomer based on PEO-R-MA-40 with a reactive C═C double bond was not only used as a surfactant but it also participated polymerization as a comonomer in aqueous media.[33] Moreover, the formation of covalent bonds between MMA and the PEO-R-MA-40 with long hydrophilic tails increased the steric stabilization. Thus, the stability of the miniemulsion polymerization can be greatly improved. On the other hand, the fluorescent vinylic crosslinking monomer (FBP), with an unsaturated double bond, copolymerized with vinyl monomers to form a covalent bond in the polymer matrix.[39,40] Importantly, this can effectively avoid the dye leakage, which is an undesired effect observed with nanoparticles when the dyes were non-covalently incorporated into the polymeric nanoparticles.[16,17] For the preparation of the photoswitchable fluorescent nanoparticles dispersion, we first synthesized a green fluorescent dye (FBP) and a photochromic spiropyran derivative (SPMA), as described in the experimental section. In order to synthesize the particle-based photoswitchable FRET system, first a mixture containing the monomers and co-surfactant (MMA, HD, FBP, SPMA) were dispersed into water with the polymerizable nonionic surfactant (PEO-R-MA-40) under ultrasonic shear force, then the water-soluble initiator (KPS) was used to start the miniemulsion polymerization. Finally, nanoparticles dispersion with covalently incorporated two dyes was produced. The as-prepared fluorescent nanoparticles dispersion display typical reversible photoswitchable fluorescence by alternately irradiating with UV/visible light in aqueous media, as illustrated in Scheme 2.

Polymer particles can be synthesized in many monodisperse sizes by adopting miniemulsion polymerization. The size of polymer particles can be controlled by changing some factors such as the amount of surfactant and hydrophobe, the concentration of monomer in aqueous solution, as well as the ultrasonication time.[21] The spectral properties of the fluorescent nanoparticles can be affected by the particle size due to the scattering of light (wavelength = $\lambda$) by a particle being at its maximum when the diameter of the particle is one half of the wavelength of incident light.[45] Thus, nanoparticles with a smaller size should be prepared to reduce the scattering effect. In this work, The averaged particle diameter ranged from *ca.* 170 nm to *ca.* 240 nm, depending on the amount of surfactant (PEO-R-MA-40) used. Specifically, for sample NP-F4, at 1 : 4 weight ratio of PEO-R-MA-40 to MMA, we can obtain a stable nanometre-sized particles with diameters down to approximately 175 nm, as determined by dynamic light scattering (DLS; see Table S1 (ESI)†). However, if we continue to increase the amount of surfactant at 1 : 2 weight ratio of PEO-R-MA-40 to MMA, we can't get a stable particle dispersion any more. In order to fabricate relatively small size polymer particles, the concentration of PEO-R-MA-40 used in this work is larger than its critical micelle concentration (CMC),[33] which means it was difficult to avoid the formation of the micellar nucleation during the polymerization process. However, in our system, the co-stabilizer used (hexadecane), which can provide sufficient osmotic pressure to counterbalance the diffusion of monomer from smaller to larger droplet (Ostwald ripening), will be helpful to form a stable miniemulsion.[23] Moreover, consideration of density variation between monomer and polymer, the little change in droplet/particle size (see Fig. S4) before and after polymerization significantly demonstrated our polymerization process is a typical miniemulsion polymerization, in which the monomer droplet nucleation is the dominant nucleation mechanism, and the micellar nucleation can be neglected.[29]

Fig. 1 shows the atomic force microscopy (AFM) of a photoswitchable fluorescent nanoparticle sample NP-N1. AFM observation revealed that most of the particles from the sample were discrete, smooth, and regular with 110–130 nm diameters. In addition, the hydrodynamic diameter for the same nanoparticle sample (NP-N1) determined by dynamic light scattering (DLS) is 175 nm (Table 1). It can be seen that the diameter of the nanoparticles determined by AFM is smaller than that of DLS analysis, this might be ascribed that the DLS measurements were carried out in solution, while the nanoparticles were somewhat made on dry solid in AFM experiments, this difference may lead

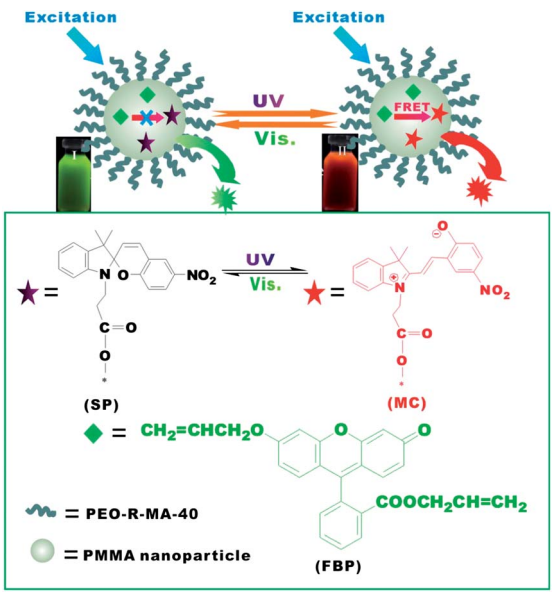


**Scheme 2** Schematic illustration of novel amphiphilic reversible photoswitchable fluorescent nanoparticles *via* covalently incorporating fluorescent dye (FBP) and photochromic derivative (SPMA).

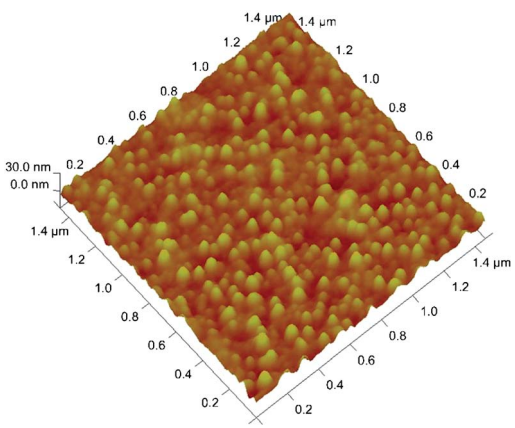


**Fig. 1** AFM image of photoswitchable fluorescent nanoparticles (sample NP-N1).

**Table 1** List of some data and parameters for two dye-incorporated nanoparticle samples

| | FBP/mg ($\times 10^{-4}$ M) | | SPMA/mg ($\times 10^{-3}$ M) | | |
|---|---|---|---|---|---|
| Sample[a] | Feed | Determined[b] | Feed | Determined[c] | Diameter[d]/nm |
| NP-N0 | 0 | 0 | 0 | 0 | 182.1 |
| NP-N1 | 2(3.96) | 1.75(3.47) | 5(0.85) | 4.4(0.75) | 172.2 |
| NP-N2 | 2(3.96) | 1.71(3.39) | 10(1.69) | 8.9(1.50) | 177.1 |
| NP-N3 | 2(3.96) | 1.69(3.35) | 15(2.54) | 12.9(2.18) | 165.4 |
| NP-S | 0 | 0 | 15(2.54) | 13.3(2.25) | 177.9 |

[a] The MMA/HD/PEO-R-MA-40/KPS feed is 0.5/0.05/0.125/0.007 g, respectively. [b] Calculated by using the absorbance of FBP at 458 nm in nanoparticle dispersion (eliminate the effect of scattering light) and the molar extinction coefficient of FBP in dichloromethane, ($\varepsilon = 25000$ mol$^{-1}$ L cm$^{-1}$). [c] Calculated by using the absorbance of SPMA at 340 nm in nanoparticle dispersion (eliminate the effect of scattering light) and the molar extinction coefficient of SPMA in dichloromethane ($\varepsilon = 8780$ mol$^{-1}$ L cm$^{-1}$). [d] Average nanoparticle diameter, determined from DLS data.



to solvent-induced swelling of the soft amphiphilic polymer nanoparticles. The above results demonstrated that uniform amphiphilic polymer nanoparticles with defined size can be prepared by miniemulsion polymerization.

### Spectroscopic properties of amphiphilic reversible photoswitchable fluorescent nanoparticles

Fig. 2 shows the absorption and fluorescence emission spectra of FBP dye in different environments, such as pure water, dichloromethane solution and a nanoparticle dispersion sample (NP-N3). As seen in Fig. 2, the maximum absorption wavelength and fluorescent emission spectra of FBP dye contained in nanoparticles and in dichloromethane are identical, indicating that the fluorophore is located within the hydrophobic polymer matrix.[17,21] To determine whether the FBP molecules were covalently incorporated in nanoparticles, the collected dried nanoparticles containing only FBP dye were repeatedly three-fold reprecipitation from dichloromethane by ether to remove the unreacted FBP dye.[39,40] The observed maximum absorptions ($\lambda_{max}$) were the same as those of the corresponding chromophores, without any noticeable batho- or hypsochromic shift indicating that no changes occurred in the basic chromophores, neither during the polymerization process, nor as a result of their inclusion in the polymer chain (see Fig. S5, (ESI)†).[39,40] On this basis, we can conclude that the FBP molecules have been chemically bonded into the nanoparticles, and by comparing the absorbance value,[39,40] it can be found that over 80% of the initially introduced dyes were covalently bound to the polymer chains.

On the other hand, it has been well documented that spiropyran can assume one of two stable states: the open-ring state, known as merocyanine (MC) state, and the closed-ring state, known as spiro (SP) state (Scheme 2).[9,10,16] In Fig. 2A, upon visible light irradiation, spiropyran moieties in the nanoparticles assumed the SP state and exhibited no absorption from 530 to 650 nm; However, after UV irradiation, a new absorbance band in the range of 530 to 650 nm appeared, which can be ascribed to the isomerization of the SP form to the MC form. The above results reveal the spiropyran derivate have also been successfully covalently incorporated into the nanoparticles. The amount of the FBP dye and spiropyran molecules in the nanoparticle dispersion given in Table 1 can be deduced by using the absorbance values assuming that the molar extinction coefficient of FBP dye and spiropyran derivate in nanoparticles is the same as that in a certain organic solution (see Fig. S6, (ESI)†).[17,21]

By changing the content (concentration) of fluorescent dye in nanoparticles, the fluorescence intensity of the nanoparticles dispersion can be correspondingly varied.[10,17,21] In this work, four different nanoparticle samples were selected to investigate the relationship between the content of fluorophores and the fluorescence intensity of the nanoparticle dispersions, as illustrated in Fig. 3. With increasing FBP content in nanoparticles, the fluorescent intensity first increases and then decreases. For the nanoparticle dispersion (FBP-3 mg) with the highest FBP concentration, its fluorescence intensity is much lower than that

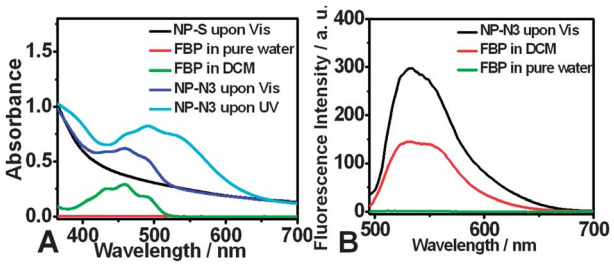


**Fig. 2** (A) Absorption spectra of FBP dye in pure water, in dichloromethane solution and in a photoswitchable fluorescent nanoparticle dispersion sample (NP-N3), as well as SPMA contained nanoparticle dispersion upon visible light (NP-S). (B) Fluorescence emission spectra of FBP dye in pure water, in dichloromethane solution and in sample NP-N3.

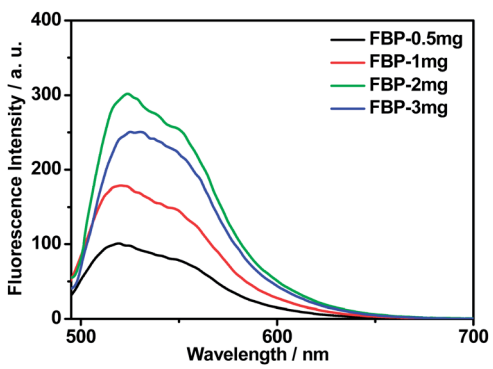


**Fig. 3** Fluorescence emission spectra for FBP dye in nanoparticle samples with different FBP feed contents.

of FBP-2 mg, and its emission maximum displays a slight red shift (~8 nm). The decreased fluorescence intensity may be caused by self-quenching of fluorescence caused by the interaction of the fluorophores, and the significant red shift of the maximum emission wavelength may be due to the formation of excited-state complex of two identical fluorophores, which takes place as the concentration of dye molecules inside the nanoparticles reaches a certain value.[46] Therefore, the appropriate amount of fluorophore should be incorporated into nanoparticles to ensure high fluorescence intensity and at the same time to avoid fluorescence self-quenching.

The effect of varying the particle size on the fluorescence intensity of nanoparticle dispersions was also investigated, as shown in Fig. 4. For these particle samples (NP-F1–NP-F4, see Table S1, (ESI)†), the concentration of FBP in the particles was kept almost identical, however, with increasing particle size, the fluorescent intensity of the dispersions decreases. The occurrence of above phenomenon, we think, may be caused by the light scattering effect of the colloidal particles. It has been shown that the light scattering can reduce the actual number of photon of the incident light received by fluorescent dyes, and the larger the particles, the stronger the light scattering effect.[21] Therefore, to ensure stronger fluorescence intensity, the particles with smaller size are preferably synthesized.

### Study of the energy transfer between donor and acceptor dyes within the nanoparticle

As for the photoreversible fluorescence modulation by using the dyad strategy,[47] the emissive behavior of the donor–acceptor (fluorophore-spiropyran or other photochromes) dyads can be varied through the intramolecular FRET, as long as the emission band of the fluorophore (donor) and the absorption band of the photochrome (acceptor) can overlap well with one of the two states of the spiropyran fragment, and the distance between the fluorophore to the spiropyran moiety should be within the Förster radius (generally, 1 nm to 10 nm).[47] For these dyad systems, the distance between the energy donor and the acceptor can be controlled by inserting a spacer between them (generally, 1 nm to 10 nm). In this work, the emission band of the fluorophore FBP (495–650 nm) excellently matches the absorption band of the MC state of spiropyran (495–650 nm) in

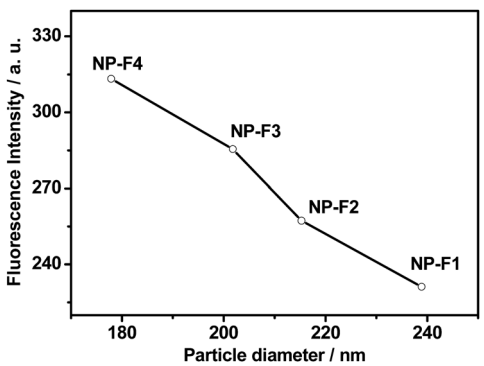


**Fig. 4** Relationship between fluorescence intensity and particle size for four nanoparticle samples. The detailed data of sample NP-F1 to NP-F4 are listed in Table S1 (ESI).†

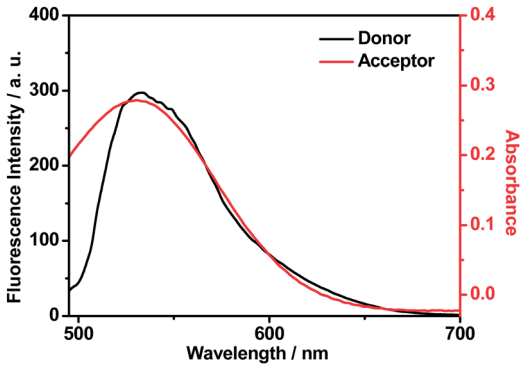


**Fig. 5** Fluorescence emission spectrum of FBP (black solid curve) and absorption spectrum of the MC form of spiropyran moieties (red solid curve) in nanoparticles.

nanoparticles (Fig. 5). Thus, these data indicate that the FRET process can take place between the FBP and the MC form of SPMA. Moreover, from the perspective of an energy-level match, the energy of the first-excited singlet state of FBP was estimated to be 2.34 eV.[47] Similar calculations based upon absorption and emission maxima gave a first-excited singlet-state energy of 3.65 eV for the SP form of the SPMA in nanoparticles, and 2.05 eV for the MC form of the SPMA.[16,47] These data also indicate that energy transfer from FBP to the SP form of SPMA is impossible, whereas that from FBP to the MC form is possible.

### Photoreversible modulation (switching) of fluorescence of nanoparticle dispersion

Fig. 6 displays modulations of fluorescence intensity of FBP by the structural interconversion of spiropyran moieties inside nanoparticles upon UV and visible light irradiation. After these nanoparticle dispersions were irradiated with UV light (300 nm, 15 W), the characteristic fluorescence emission for FBP at 531 nm considerably decreases, and a new emission band at *ca.* 640 nm appeared, which can be attributed to the MC form of SPMA moieties. However, with the irradiation of visible light (525 nm, 15 W LED lamp), the fluorescence intensity was recovered (Fig. 6). In addition, the appearance of fluorescence from aqueous nanoparticles dispersion can also be reversibly modulated by alternately irradiating with UV/visible light, as shown in Fig. 7. It can be seen that the color of the nanoparticle dispersion (NP-N3) turns into red after UV irradiation and reverts to green after visible light illumination. The red color corresponds to the MC form of spiropyran moieties in the nanoparticles while the green corresponds to the FBP dye.

On the basis of the results in Fig. 6, the fluorescence intensity of FBP can be remarkably quenched by the MC form of SPMA moieties through an intraparticle FRET process, According to the Förster nonradiative energy transfer theory,[47,48] the Förster's critical distance $R_0$ between the FBP (donor) and the acceptor (MC) in nanoparticles has been calculated to be 45.1 Å (see (ESI)†). The FRET efficiency $E$ is expressed as:

$$E = \frac{R_0^6}{R_0^6 + r^6} \quad (1)$$

where $r$ is the distance between the donor (FBP) and the acceptor (MC form of SPMA). The energy transfer is effective over

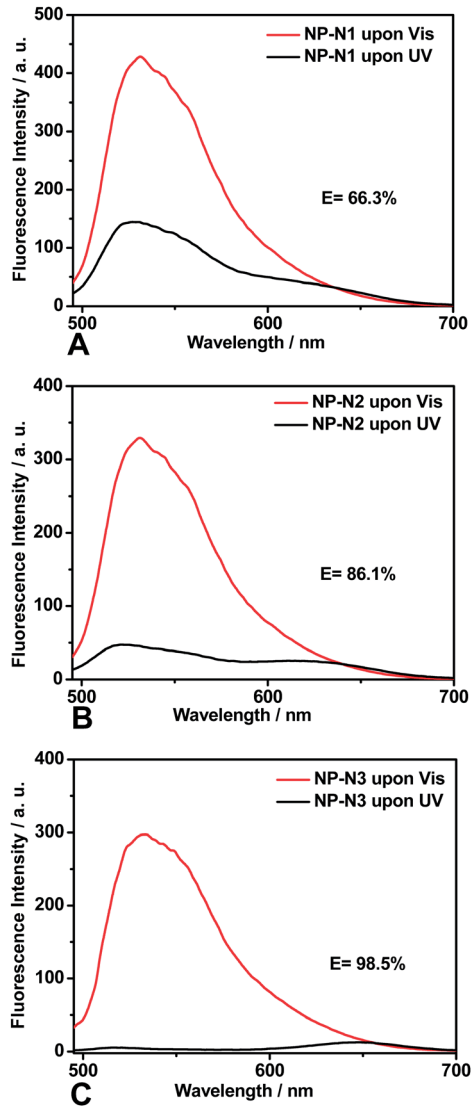


**Fig. 6** Fluorescence emission spectra (excited at 480 nm, 25 °C) of photoswitchable fluorescent nanoparticle dispersions modulated by UV irradiation (300 nm) or by visible light (525 nm) irradiation. The concentration for FBP is $6.7 \times 10^{-5}$ M in aqueous dispersion and that for the spiropyran moiety is $1.5 \times 10^{-4}$ M (sample NP-N1, spiropyran feed: 0.005 g) (A), $3.0 \times 10^{-4}$ M (sample NP-N2, spiropyran feed: 0.010g) (B), $4.4 \times 10^{-4}$ M (sample NP-N3, spiropyran feed: 0.015 g) (C) respectively.

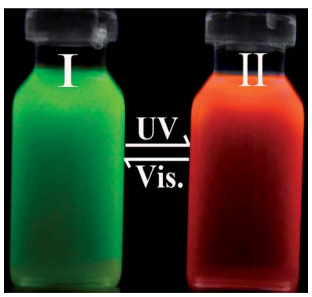


**Fig. 7** Photograph of a nanoparticle dispersion (NP-N3) after visible light irradiation (I) and UV irradiation (II) under the dark environment and UV excitation.

distances in the $R_0 \pm 50\%$ $R_0$ range,[47] namely, 22.6 Å $\leq r \leq$ 67.6 Å. However, unlike the dyad systems, the FBP dye molecules and spiropyran moieties are dispersed in the PMMA core particles and separated by the polymer matrix, and the distance between donor and acceptor is governed by the amount of donors and acceptors incorporated in the individual nanoparticles assuming the fluorophores are uniformly dispersed.

For the amphiphilic core–shell nanoparticles, the average diameter of the nanoparticles can roughly be calculated by the AFM, as shown in Table 2. In this study, because two dyes were resided in hydrophobic PMMA core of amphiphilic nanoparticles, we need to estimate the average diameter of nanoparticle core ($D_{core}$, see ESI†), then we can calculate the average number of FBP ($N_{FBP}$/NP) and spiropyran ($N_{SP}$/NP) in a nanoparticle core, the average ratio of spiropyran number to FBP number in one nanoparticle core ($N_{SP}/N_{FBP}$), the experimental energy transfer efficiency ($E$) for the nanoparticle samples as well as the estimated average distance between FBP and spiropyran in nanoparticles ($r$) for the samples, and listed the data in Table 2. In addition, it should be considered that the energy can be transferred from a donor to an acceptor if their separation distance is less than the upper limit of efficient energy transfer (67.6 Å). Thus, we also estimated the number of the spiropyran ($N_A$) residing around one donor within the effective energy transfer distance, assuming that the dispersion of spiropyran molecules or FBP molecules in the whole nanoparticle core is homogeneous, and the existence of the donor (FBP) does not affect the dispersion of the acceptor (spiropyran) and *vice versa*, and listed the data ($N_A$) in Table 2.

The data shown in Table 2 indicate that for the three nanoparticle samples from NP-N1 to NP-N3, with the irradiation of UV light, in most of the samples there are multiple acceptors (MC) around a donor within the effective energy transfer distance of 67.6 Å, this ensures the intraparticle FRET process takes place from donor to acceptor as well as the light-induced fluorescent modulation. Moreover, for the nanoparticle samples with higher ratio of spiropyran to FBP (NP-N3), there are more MC molecules around a FBP molecule (donor), and higher experimental energy transfer efficiency can be achieved; while for the sample with the lowest ratio of spiropyran to FBP (NP-N1), averagely there are only 15.5 effective acceptors (MC) around a FBP within 67.6 Å, and the experimental energy transfer efficiency is 66.3% and the fluorescence emission of FBP cannot be effectively quenched under the UV-light irradiation, as illustrated in Fig. 5A. Under the current experimental conditions, the critical $N_{spiropyran}/N_{FBP}$ value, which ensures effective fluorescence quenching ($E = 98.5\%$), is estimated to be 49.6. Moreover, the control of the acceptor to donor ratio during the polymerization is important to obtain nanoparticles dispersion with well-defined energy transfer efficiency as well as fluorescence emission properties.

Fig. 8A shows typical fluorescence response behavior of the aqueous dispersion of fluorescent nanoparticles containing only FBP dye (NP-F4) and the novel photoswitchable fluorescent nanoparticles (NP-N3) with irradiation of UV and visible light. As depicted in Fig. 8A, the changes in fluorescence intensity of nanoparticles dispersion containing only FBP at 531 nm are not apparent, thus, its photodegradation is neglectable in such short-time irradiation by low energy (15 W) UV or visible light.

**Table 2** Characteristics of three FBP and spiropyran-containing nanoparticle samples

| Sample[a] | $D_{NP}$[b] (nm) | $C_{FBP}$[c] ($\times 10^{-4}$ M) | $N_{FBP}$/NP | $C_{SP}$[c] ($\times 10^{-3}$ M) | $N_{SP}$/NP | $N_{SP}/N_{FBP}$ | $N_A$[d] | $E$ (%)[e] | $r$[f] nm |
|---|---|---|---|---|---|---|---|---|---|
| NP-N1 | 147.6 | 3.47 | 8387 | 0.75 | 16129 | 1.9 | 15.5 | 66.3 | 4.03 |
| NP-N2 | 146.1 | 3.39 | 7813 | 1.50 | 34375 | 4.4 | 33.1 | 86.1 | 3.32 |
| NP-N3 | 142.1 | 3.35 | 7143 | 2.18 | 45714 | 6.4 | 49.6 | 98.5 | 2.09 |

[a] The MMA/HD/PEO-R-MA-40/KPS feed is 0.5/0.05/0.125/0.007g, respectively. [b] $D_{NP}$: average nanoparticle diameter, obtained by AFM. [c] $C_{FBP}$ and $C_{spiropyran}$: mole concentration of FBP and spiropyran in dispersion respectively, determined from the absorbance values. [d] The number of spiropyran residing around one donor (FBP) within the effective energy transfer distance (see (ESI)†). [e] The experimental energy transfer efficiency (see (ESI)†). [f] The estimated average FBP-spiropyran distance (see (ESI)†).



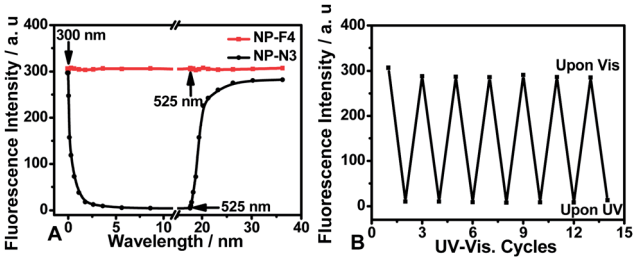


**Fig. 8** Fluorescence response (excitation at 480 nm and emission at 531 nm) of only FBP-containing fluorescent nanoparticle dispersion and photoswitchable fluorescent nanoparticle dispersion (sample NP-N3) upon irradiation with 300 nm UV and 525 nm visible light (15 W) (A); and fluorescence intensity change at 531 nm for the nanoparticle sample NP-N3 after UV illumination and visible light irradiation cycles (B).

However, for the sample NP-N3, upon UV irradiation, the fluorescence intensity of FBP moieties at 531 nm abruptly decreases within 10 min and then tends towards stability, indicating a quenching by the ring-opened MC form of SPMA. While it gradually recovers its fluorescence intensity upon irradiation with 525 nm visible light within 20 min, which can be ascribed to the photoinduced conversion from MC form to SP form of spiropyran moieties. The FRET process between FBP and SPMA residues can be reversibly switched "on" and "off" by cyclically irradiating with UV and visible light (Fig. 8B). As seen from the fact that the optical switching of fluorescence can be repeated for six cycles with a slight "fatigue" effect.[49] Obviously, the novel nanoparticles prepared by employing covalent bonding strategy possess better resistance to fatigue when compared to our previous photoswitchable systems, in which dye molecules are incorporated by doping or adsorbing to the polymeric matrix.[16]

## Conclusion

In conclusion, two energy level well-matched fluorophores, fluorescein-based crosslinking monomer, fluorescein-*O*,*O*-bis-propene (FBP) and spiropyran-linked methacrylate (SPMA) have been successfully covalently incorporated into the polymer nanoparticles by a facile one-pot miniemulsion polymerization using a polymerizable nonionic surfactant, ω-methoxy poly (ethylene oxide) undecyl α-methacrylate (PEO-R-MA-40), forming nanoparticle-based optically addressable two-color fluorescent systems in aqueous media. There is no dye leakage for nanoparticles because of the covalent incorporation of dye molecules. The fluorescence emission of FBP dye in nanoparticles can be reversibly modulated by the transformation of the spiropyran moieties structures upon irradiation with UV and visible light. Overall, the resulting novel amphiphilic reversible photoswitchable fluorescent nanoparticles not only show controllable amount and ratio of the two dyes, high fluorescence intensity, and tunable FRET efficiency, but also exhibit excellent photostability, relatively fast photoresponsibility, and better photoreversibility compared to some previous reports. This class of novel FRET-mediated photoresponsive nanoparticles may have a variety of interesting applications in biological labeling and imaging.

## Acknowledgements

This work was supported by NSFC (Project No. 51003026, and 21172066), Hunan Provincial Natural Science Foundation of China (NO.11JJ4016) and the Open Project Program of Key Laboratory of Advanced Functional Polymeric Materials (Xiangtan University), College of Hunan Province (No. AFPM200907).

## Notes and references

1 F. Zhang, G. B. Braun, Y. Shi, Y. Zhang, X. Sun, N. O. Reich, D. Zhao and G. Stucky, *J. Am. Chem. Soc.*, 2011, **132**, 2850.
2 S. Santra, R. P. Bagwe, D. Dutta, J. T. Stanley, G. A. Walter, W. Tan, B. M. Moudgil and R. A. Mericle, *Adv. Mater.*, 2005, **17**, 2165.
3 H. N. Kim, Z. Guo, W. Zhu, J. Yoon and H. Tian, *Chem. Soc. Rev.*, 2011, **40**, 79.
4 S. Santra, H. Yang, D. Dutta, J. T. Stanley, P. H. Holloway, W. H. Tan, B. M. Moudgil and R. A. Mericle, *Chem. Commun.*, 2004, 2810.
5 S. T. Selvan, T. T. Y. Tan, D. K. Yi and N. R. Jana, *Langmuir*, 2010, **26**, 11631.
6 Z. Tian, W. Wu and A. D. Q. Li, *ChemPhysChem*, 2009, **10**, 2577.
7 P. Sharrna, S. Brown, G. Walter, S. Santra and B. Moudgil, *Adv. Colloid Interface Sci.*, 2006, **123**, 471.
8 E. Rampazzo, S. Bonacchi, M. Montalti, L. Prodi and N. Zaccheroni, *J. Am. Chem. Soc.*, 2007, **129**, 14251.
9 S. Z. Wu, Y. L. Luo, F. Zeng, J. Chen, Y. N. Chen and Z. Tong, *Angew. Chem., Int. Ed.*, 2007, **46**, 7015.
10 N. Shao, J. Y. Jin, S. M. Cheung, R. H. Yang, W. H. Chan and T. Mo, *Angew. Chem., Int. Ed.*, 2006, **45**, 4944.
11 D. M. Chudakov, V. V. Verkhusha, D. B. Staroverov, E. A. Souslova, S. Lukyanov and K. A. Lukyanov, *Nat. Biotechnol.*, 2004, **22**, 1435.
12 R. Ando, H. Mizuno and A. Miyawaki, *Science*, 2004, **306**, 1370.
13 J. Cusido, E. Deniz and F. M. Raymo, *Eur. J. Org. Chem.*, 2009, 2031.
14 X. J. Zhao, R. Tapec-Dytioco and W. H. Tan, *J. Am. Chem. Soc.*, 2003, **125**, 11474.
15 S. T. Selvan, T. T. Tan and J. Y. Ying, *Adv. Mater.*, 2005, **17**, 1620.
16 J. Chen, F. Zeng, S. Z. Wu, Q. M. Chen and Z. Tong, *Chem.–Eur. J.*, 2008, **14**, 4851.

 

17 M. Frigoli, K. Ouadahi and C. Larpent, *Chem.–Eur. J.*, 2009, **15**, 8319.
18 L. Y. Zhu, W. W. Wu, M. Q. Zhu, J. J. Han, J. K. Hurst and A. D. Q. Li, *J. Am. Chem. Soc.*, 2007, **129**, 3524.
19 J. Fölling, S. Polyakova, V. Belov, A. van Blaaderen, M. L. Bossi and S. W. Hell, *Small*, 2008, **4**, 134.
20 T. Wu, G. Zou, J. Hu and S. Liu, *Chem. Mater.*, 2009, **21**, 3788.
21 J. Chen, P. S. Zhang, G. Fang, P. G. Yi, X. Y. Yu, X. F. Li, F. Zeng and S. Z. Wu, *J. Phys. Chem. B*, 2011, **115**, 3354.
22 D. Crespy, A. Musyanovych and K. Landfester, *Colloid Polym. Sci.*, 2006, **284**, 780.
23 K. Landfester, *Top. Curr. Chem.*, 2003, **227**, 75.
24 P. Ni, M. Zhang, L. Ma and S. Fu, *Langmuir*, 2006, **22**, 6016.
25 W. Li, K. Min, K. Matyjaszewski, F. Stoffelbach and B. Charleux, *Macromolecules*, 2008, **41**, 6387.
26 S. Lu, J. Ramos and J. Forcada, *Langmuir*, 2007, **23**, 12893.
27 R. Faridi-Majidi and N. Sharifi-Sanjani, *J. Appl. Polym. Sci.*, 2007, **106**, 3515.
28 F. Tiarks, K. Landfester and M. Antonietti, *Langmuir*, 2001, **17**, 908.
29 C. S. Chern and Y. C. Liou, *Polymer*, 1999, **40**, 3763.
30 D. Cochin, A. Laschewsky and F. Nallet, *Macromolecules*, 1997, **30**, 2278.
31 R. H. Ottewill and R. Satgurunathan, *Colloid Polym. Sci.*, 1995, **273**, 379.
32 A. Guyot, *Curr. Opin. Colloid Interface Sci.*, 1996, **1**, 580.
33 J. Liu, C. H. Chew, L. M. Gan, W. K. Teo and L. H. Gan, *Langmuir*, 1997, **13**, 4988.
34 J. Liu, C. H. Chew and L. M. Gan, *J. Macromol. Sci., Part A: Pure Appl. Chem.*, 1996, **33**, 337.
35 J. Liu, C. H. Chew, S. Y. Wong, L. M. Gan, J. Lin and K. L. Tan, *Polymer*, 1998, **39**, 283.
36 J. Liu, L. M. Gan, C. H. Chew, C. H. Quek, H. Gong and L. H. Gan, *J. Polym. Sci., Part A: Polym. Chem.*, 1997, **35**, 3575.
37 J. Liu, L. M. Gan, C. H. Chew, W. K. Teo and L. H. Gan, *Langmuir*, 1997, **13**, 6421.
38 J. Liu, W. K. Teo, C. H. Chew and L. M. Gan, *J. Appl. Polym. Sci.*, 2000, **77**, 2785.
39 T. N. Konstantinova and V. B. Bojinov, *Dyes Pigm.*, 1998, **39**, 69.
40 T. Konstantinova, G. Kirkova and R. Betcheva, *Dyes Pigm.*, 1998, **38**, 11.
41 P. Meallier, S. Guittonneau, C. Emmelin and T. Konstantinova, *Dyes Pigm.*, 1999, **40**, 95.
42 T. Konstantinova, G. Cheshmedjieva-Kirkova and H. Konstantinov, *Polym. Degrad. Stab.*, 1999, **65**, 249.
43 T. Konstantinova and G. Cheshmedjieva-Kirkova, *Polym. Degrad. Stab.*, 2000, **70**, 77.
44 A. Fissi, O. Pieroni, G. Ruggeri and F. Ciardelli, *Macromolecules*, 1995, **28**, 302.
45 K. Ando and H. Kawaguchi, *J. Colloid Interface Sci.*, 2005, **285**, 619.
46 W. Wang, J. J. Han, L. Q. Wang, L. S. Li, W. J. Shaw and A. D. Q. Li, *Nano Lett.*, 2003, **3**, 455.
47 J. Chen, F. Zeng and S. Z. Wu, *ChemPhysChem*, 2010, **11**, 1036.
48 J. R. Lakowicz, *Principles of Fluorescence Spectroscopy*, Springer, New York, 2006.
49 G. Baillet, G. Giusti and R. Guglielmetti, *J. Photochem. Photobiol., A*, 1993, **70**, 157.